https://doi.org/10.5194/egusphere-2025-4175
Preprint. Discussion started: 12 September 2025

A Fracture Never Comes Alone: Associations of Fractures and Stylolites in Analogue Outcrops Improve Borehole Image Interpretations of Fractured Carbonate Geothermal Reservoirs

Jasper Hupkes[1], Pierre-Olivier Bruna[1], Giovanni Bertotti[1], Myrthe Doesburg[1], and Andrea Moscariello[2]
[1]Department of Geoscience and Engineering, Delft University of Technology, Delft, The Netherlands
[2]Department of Earth Sciences, University of Geneva, Geneva, Switzerland
Correspondence: Jasper Hupkes (j.hupkes@tudelft.nl)

Abstract. Natural discontinuity networks control convective fluid flow in carbonate geothermal reservoirs with low matrix porosity and permeability. The network can be separated into discontinuities that formed due to local drivers (e.g. faults/folds) and the background network formed by far-field stresses, each with different scaling behaviour. Borehole data are the only source to sample the subsurface network, as the majority of the discontinuities are of sub-seismic scale. Borehole images are the most cost-effective way of sampling the network, but the limited sample area and image resolution hamper the identification of the background network in this dataset. Analogue outcrops may complement the borehole data, but only after the analogy between outcrop and subsurface reservoir is established. In this study, we present a method that uses associations of discontinuity sets to establish a robust link between the outcrop and the subsurface. A discontinuity association comprises up to 4 discontinuity sets that can form coeval in a single stress field, a well-known concept that is rarely applied for subsurface characterization of discontinuities. We use the orientations and type of discontinuity associations as paleostress indicators in order to map out principal stress trajectories of regional discontinuity-forming events that created the background discontinuity network. We demonstrate this methodology in the Geneva Basin, Switzerland, where the naturally fractured Lower Cretaceous pre-foredeep carbonates are targeted for geothermal exploitation. Outcrops in the mountain ranges that surround the basin, consistently reveal two multiscale discontinuity-forming events that formed prior to Alpine fold-and-thrusting and thus constitute the regional scale background network. Therefore, based on the analogy principle, we predict that the target reservoir is also affected by these events. We use this prediction to isolate background-related discontinuities on image logs from two boreholes that penetrate the target reservoir in the Geneva Basin. This analysis reveals that ∼45% of the observed discontinuities can be understood in the framework of the regional-scale background. In this way, we demonstrate that DAs in outcrops are a powerful tool to predict the geometry of natural discontinuity networks in the subsurface and subsequently can be used to develop geothermal exploitation strategies in naturally fractured reservoirs.

1 Introduction

Natural discontinuity networks (NDNs) control convective heat flow in fractured geothermal reservoirs with a low matrix porosity and permeability (Berre et al., 2019; Medici et al., 2023). Discontinuities can create a heterogeneous reservoir perme-

https://doi.org/10.5194/egusphere-2025-4175
Preprint. Discussion started: 12 September 2025

ability by either forming preferred flow pathways or flow barriers (Bruna et al., 2019; La Bruna et al., 2021). Predicting the geometry of NDNs in the subsurface is crucial to avoid production risks such as early thermal breakthrough (Fadel et al., 2023) and/or induced seismicity (Zang et al., 2014; Atkinson et al., 2020).

A common approach to analyze NDNs is by breaking the network down into discontinuity sets (Peacock et al., 2018). The definition of a set is based on the orientation of the discontinuities and, if possible to determine, the discontinuity type. These sets can be separated based on their geomechanical driver. Their formation is either related to local drivers such as folds and faults (Price, 1966; Torabi and Berg, 2011) or to regional, far-field stresses (Lamarche et al., 2012; Bertotti et al., 2017; Lavenu and Lamarche, 2018; La Bruna et al., 2020). Discontinuities formed by the latter constitute the background network. The spatial distribution of the intensity of the discontinuities is partially controlled by the driver. For local drivers, discontinuities concentrate where strain accumulates (e.g. in the damage zone or fold hinge), whereas the background network is more homogeneously distributed.

The majority of the discontinuities are of sub-seismic scale. Seismic data can aid the prediction of the sub-seismic discontinuities in the subsurface related to local drivers, if faults and/or folds are above the seismic resolution (Maerten et al., 2006). Predicting the background network based on seismic data however remains challenging, as there are no seismic-scale structures related to this part of the network. The only way to directly observe sub-seismic scale discontinuities of the background network in the subsurface is through borehole data. These data classically consist of cores and borehole images. Borehole images (BHI) are a cost-effective alternative to core data, enabling classification of discontinuities based on their structural attitude (dip and strike) and their geophysical responses (filled – resistive or open - transmissive) (Williams and Johnson, 2004). However, the resolution of BHIs may hinder the identification of discontinuity type, which is crucial to interpret the geomechanical driver of the discontinuity. On top of this, the sampling area (diameter of the borehole) is too small to observe the relationship between individual discontinuities and local structures such as faults and folds. This prevents the separation in the borehole of background-related discontinuities from those that formed due to local stresses.

In contrast, outcrop studies allow to characterize the key attributes of discontinuities that are necessary to retrieve the geological driver responsible of their formation. But to use the outcrop for subsurface characterization of NDNs, the analogy between the two domains needs to be established (Peacock et al., 2022). Besides similar lithology and age of formation, a shared tectonic history is important for establishing such analogy (Petit et al., 2022). As the background network is the result of regional, far-field stresses, it is likely that both outcrops and the subsurface preserved discontinuities related to these regional stresses. Therefore, the orientation of the stress field that produced the background network can potentially function as the link between outcrop and subsurface.

There are various methods that use discontinuities for paleostress inversion (Angelier, 1990; Maerten et al., 2016; Pascal, 2021). Associations of discontinuities that formed coeval in a single stress field are more robust indicators than single discontinuity sets 1 (Hancock, 1985). The concept that multiple discontinuity sets can form in a single stress field is largely sensed by structural geologist but surprisingly little used to establish the analogy between outcrop and the subsurface. This notion gives additional value to the surface study, as it may provide a geological context for the interpretation of BHI-data from the target reservoir. The derived paleo principal stresses that caused the formation of the background network as observed in the field can

https://doi.org/10.5194/egusphere-2025-4175
Preprint. Discussion started: 12 September 2025

be used to predict the orientation of discontinuities in the subsurface. Based on the predicted orientations, background-related discontinuities in the borehole can be separated from those that formed by other, local mechanisms. The regional nature of the background network allows the extrapolation of these discontinuities away from the borehole and even beyond the limits of the targeted reservoir. In this way, investigating analogue outcrops can minimize the risks of further exploitation of the targeted geothermal reservoir.

In this study, the concept of using associations of background discontinuities as the link between outcrop and target reservoir is applied to the pre-foredeep Lower Cretaceous limestone in the Geneva Basin. Recently, the Canton of Geneva supported different geothermal projects to exploit the subsurface of the Geneva Basin for cooling and heating applications (Geothermies https://www.geothermies.ch/, Heatstore https://www.heatstore.eu/). In the scope of these projects, two wells (GEo-01 and GEo-02) have recently been drilled in the basin for geothermal exploration of the Mesozoic carbonates in the basin (Guglielmetti et al., 2021). Borehole data (including borehole images) of the two wells have shown that the Lower Cretaceous formations in particular are a potential geothermal reservoir due to a high, natural fracture-related permeability (Rusillon, 2017; Brentini, 2018; Moscariello, 2019; Clerc and Moscariello, 2020; Guglielmetti and Moscariello, 2021). Outcrops of the Lower Cretaceous are found on both the northwestern, southwestern and southeastern sides of the basin (figure 2, Jura Mountains, Vuache Range and Parmelan/Salève Range respectively). In these outcrops, we isolate the discontinuities of the background network that formed due to far-field stresses, focusing only on the associations of discontinuities that formed prior to Alpine fold-and-thrusting that shaped the present-day mountain ranges. Subsequently, we reconstruct regional paleostress trajectories to establish the analogy between outcrop and target reservoir, and thus enable the prediction of the geometry of the background network in the subsurface. We use the results of the outcrop study in our discontinuity interpretation of the BHI of the two wells in the target reservoir to quantify the portion of the background network compared to the total network. The results provide valuable information for future geothermal explorations in the area.

2 Methodology

2.1 Grouping Discontinuities into Associations

Our approach is based on outcrop observations of discontinuities, namely mode I and mode II fractures, vein arrays and stylolites, that are genetically associated with a certain stress field (figure 1). Discontinuity sets are defined on the basis of both orientation and discontinuity type. A theoretically complete discontinuity association (DA) consists of four sets of discontinuities: one mode-I set, oriented perpendicular to $\sigma 3$; a conjugated pair of mode-II fractures or vein arrays, with a $\sim 60°$ to $30°$ angle respectively, bisected by $\sigma 1$; and a stylolite forming perpendicular to $\sigma 1$. In this study, mode-I and mode-II discontinuities in general are referred to as fractures. If a fracture is (partially) filled with cement, they are called veins. Veins are treated similarly as other fractures for determining DAs. In the study area, they are found as mode-I opening fractures, mode-II shear fractures, and vein arrays belonging to semi-ductile shear zones. The latter may form conjugate pairs similar to mode-II fractures (Beach, 1975).

https://doi.org/10.5194/egusphere-2025-4175
Preprint. Discussion started: 12 September 2025

Observations in the field are made per station with a size of ∼10x10 meters. We aimed to distribute the stations as evenly as possible over the studied area in order to obtain a representative dataset, but the quality of the outcrop exposure also affected the choice of the locations (Peacock et al., 2019). In each station, we document the discontinuities that can be placed into a DA. The orientation of the DAs are used to map the related paleostress directions. To ensure the robustness of the reconstructed paleostress directions, we consider a minimum of two discontinuity sets that are associated together to define a DA. For example, a stylolite together with a conjugate pair of mode-II fractures is considered a very reliable indicator. On the contrary, we discard isolated features which provide ambiguous stress information, such as isolated mode-I fractures.

This method inherently means that not all discontinuities observed are documented. To quantify how representative the defined associations are for the total network, we measured augmented circular scanlines on 7 pavements (Mauldon et al., 2001; Watkins et al., 2015a). As the Parmelan is the only outcrop providing quality pavements to conduct circular scanline analysis, all scanlines are taken there. Per pavement, a total of 4 to 12 scanlines with a radius of 1 meter are collected. The orientation and type of discontinuities that intersect the circular scanlines are documented. The qualitatively defined associations from the nearest by station are used to separate the loose features that cannot be understood in the framework of an association from those that do. This gives an indication of the portion of discontinuities that fit within the framework of associations with respect to the total network.

2.2 DAs as the link between outcrop and subsurface

The mapped paleo principals stresses per station are used to determine the stress regime in which the DA was formed (i.e. normal, reverse, or strike-slip). We assume that all DAs are formed in Andersonian stress fields (Anderson, 1905), i.e. two of the principal stresses were positioned horizontally at the timing of discontinuity formation. This is used to reconstruct the relative timing between the formation of a DA and the tilting of the strata (figure 1). If two of the three principle paleostresses are oriented parallel to the bedding, and the bedding is tilted, we infer that the DA formed prior to the tilting of the strata. The relative timing between different DAs is reconstructed based on abutment and cross-cutting relationships of individual discontinuities.

In our research area, up to 3 different DAs are observed in a single station. If the difference between the stress fields of two different DAs is only a permutation of the principle stresses, the simplest cause is a change in overburden (Bertotti et al., 2017) or by intermediate stress regimes (Simpson, 1997). Therefore, these DAs are grouped into single events. We use two criteria to define regional, background network forming events. Firstly, the relative timing of the DAs that make up the event must be prior to tilting of the strata. Secondly, the orientation of the principle stresses of the DA must be similar in all analogue outcrops, i.e. constant on a regional scale. If the two criteria are fulfilled, we predict that the target reservoir that is located between the analogue outcrops, also is affected by these regional events. The regional events we use to predict the orientation of discontinuities in the subsurface, and we use this prediction to improve the understanding of the fractures observed on BHI from drilled in the target reservoir by separating the background-related discontinuities from the total network.

https://doi.org/10.5194/egusphere-2025-4175
Preprint. Discussion started: 12 September 2025

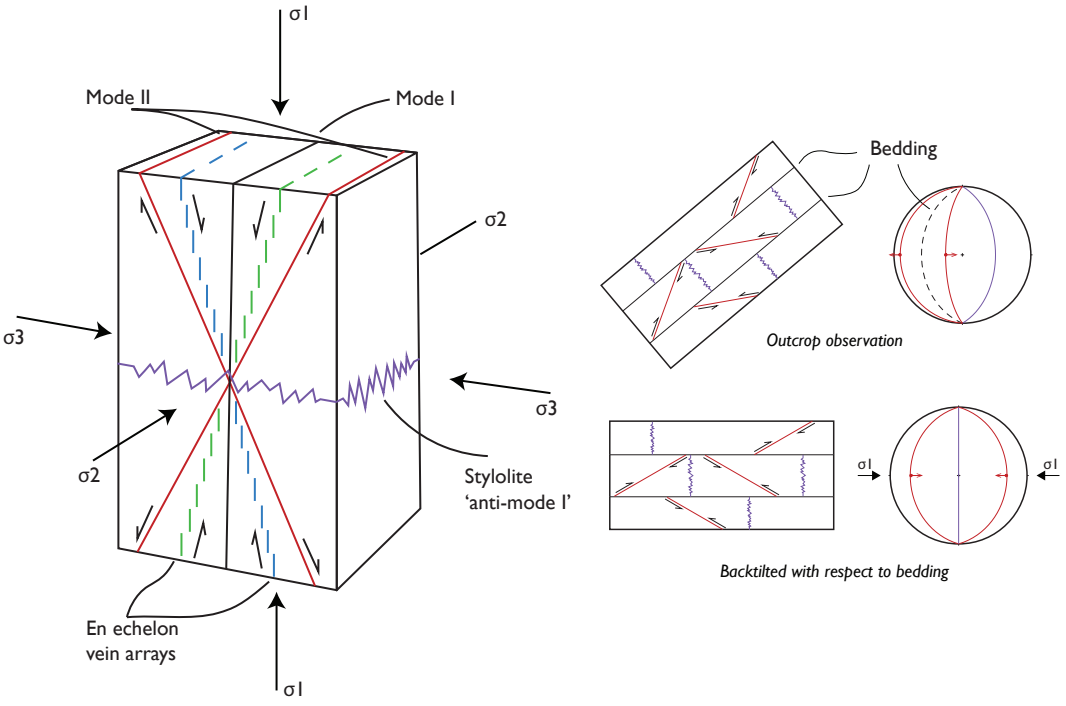

Figure 1. Left: Conceptual model illustrating a discontinuity association, adapted from Hancock (1985). There are four discontinuity sets that can form coeval in a single stress field, and are therefore in association with each other. For legenda of colours, see figure 3. Right: illustration of how the timing of the formation with respect to tilting of the bedding is deduced. After back-tilting the association with respect to the bedding, the maximum principal stress becomes horizontal. Therefore, all the discontinuities that make the set (in this case, a conjugate pair of shear fractures and a stylolite), formed prior to tilting of the strata and are thus part of the background network.

3 Geological Background

The Geneva Basin is located in the western part of the Swiss Molasse Basin/North Alpine Foreland Basin (figure 2). It is bounded by the Jura Mountains in the northwest, the Salève Range in the southeast and the Vuache range in the southwest. In the subsurface of the basin, the Mesozoic strata are dipping 10° to 20° to the southeast. The depth of the top of the Lower Cretaceous increases from surface exposures in the northwest (Jura Mountains) to ∼1400 m in the southeast at the foot of the Salève Range (Jenny et al., 1995; Guglielmetti et al., 2020).

At present-day, exposures of the Lower Cretaceous are found in the mountain ranges surrounding the Geneva Basin and the Bornes Massif, part of the Sub-Alpine Chain (figure 2). In the Bornes Massif, the Parmelan plateau contains excellent exposures of the Lower Cretaceous carbonates. The plateau of the Parmelan is located in the crest of a box-fold (Berio et al., 2021), underlain by a NW-vergent thrust (Bellahsen et al., 2014) that structurally separates it from the Salève Range in the northwest. The Salève Range is also positioned above a NW-vergent thrust that marks the southeastern boundary of the Geneva Basin (Charollais et al., 2023). The Lower Cretaceous is exposed on the SE-dipping limb of this range. On the other side of the Geneva basin, the Jura Mountains contains several Lower Cretaceous exposures. The mountain range is shaped by NW-verging

https://doi.org/10.5194/egusphere-2025-4175
Preprint. Discussion started: 12 September 2025

folds and thrust formed by thin-skinned deformation (Homberg et al., 2002; Sommaruga et al., 2017). The Vuache Fault is part of a system of sinistral strike-slip faults related to the NW-vergent thrusting in the Jura (Homberg et al., 2002; Smeraglia et al., 2022). Transpression along this fault gave rise to the Vuache Range, with several exposures of the Lower Cretaceous carbonates.

The Lower Cretaceous formations consists predominantly of carbonates, with intercalations of marl layers (Rusillon, 2017; Strasser et al., 2016). They are deposited in a branch of the Tethys Ocean (Clavel et al., 2007, 2013). Subsequently, they are buried beneath Eocene to Pliocene molasse sediments in the foredeep of the Alpine Orogeny, whose thickness tapers towards the northwest. The estimated maximal burial depths of the Lower Cretaceous range between 2000 m in the Geneva Basin (Schegg and Leu, 1998) and 4000 m in the Bornes Massif (Butler, 1991; Moss, 1992; Deville and Sassi, 2006). In the Early Miocene, shortening in the Western Alps was accommodated by different folds and thrusts with a northwest vergence (Kalifi et al., 2021; Marro et al., 2023), ultimately leading to the exhumation of the Lower Cretaceous in the present-day mountain ranges in the Pliocene (Cederbom et al., 2004).

4 Results

We documented DAs at 28 different stations in the study area. The first area we will describe is the plateau of the Parmelan, part of the Bornes Massif. Due to the superb quality of this exposure, the majority (18) of the stations are documented there. In total there are three different associations observed on the Parmelan. The stations in the Jura and Vuache are described together (9 in total). In these outcrops, a total of four different associations are defined. The third area is the Salève Range. Due to limited exposures on top of this range, only one station is recorded here, where one association is defined. All the defined associations can ultimately be grouped into two regional discontinuity forming events that formed pre-tilting of the strata.

4.1 Parmelan

Veins, stylolites and shear fractures are common on the Parmelan and can be arranged in discontinuity associations. The oldest association (PA1) is expressed by a conjugate pair of shear fractures and tectonic stylolites, observed on meter-scale. The shear fractures strike ∼045°-225° with a low dip angle with respect to the bedding (∼15°-30°). Dissolution on the shear planes makes them clearly visible on bed-perpendicular exposures (figure 3A). In some instances, slickensides are preserved on the shear planes, indicating reverse kinematics. The tectonic stylolites have a similar strike as the shear fractures, but are bed-perpendicular. The angular relationship between the shear fractures, stylolites and bedding are observed everywhere, even in the steeply dipping limbs of the box fold that shapes the Parmelan (e.g. station 18). Therefore, they are formed prior to the tilting of the strata. This association formed in a reverse stress regime with $\sigma 1$ oriented NW-SE.

The second association (PA2) comprises both small and large discontinuities, ranging from meter to kilometer in length. The smaller discontinuities are made up of two sets of sub-vertical vein arrays with opposing sense of shear (figure 3B) and tectonic stylolites. The latter similarly oriented as those of PA1. Sinistral arrays have an average strike of 150°-330°, whereas dextral arrays strike 120°-300° on average. The cement of the veins is yellow-white and have a blocky texture.

https://doi.org/10.5194/egusphere-2025-4175
Preprint. Discussion started: 12 September 2025

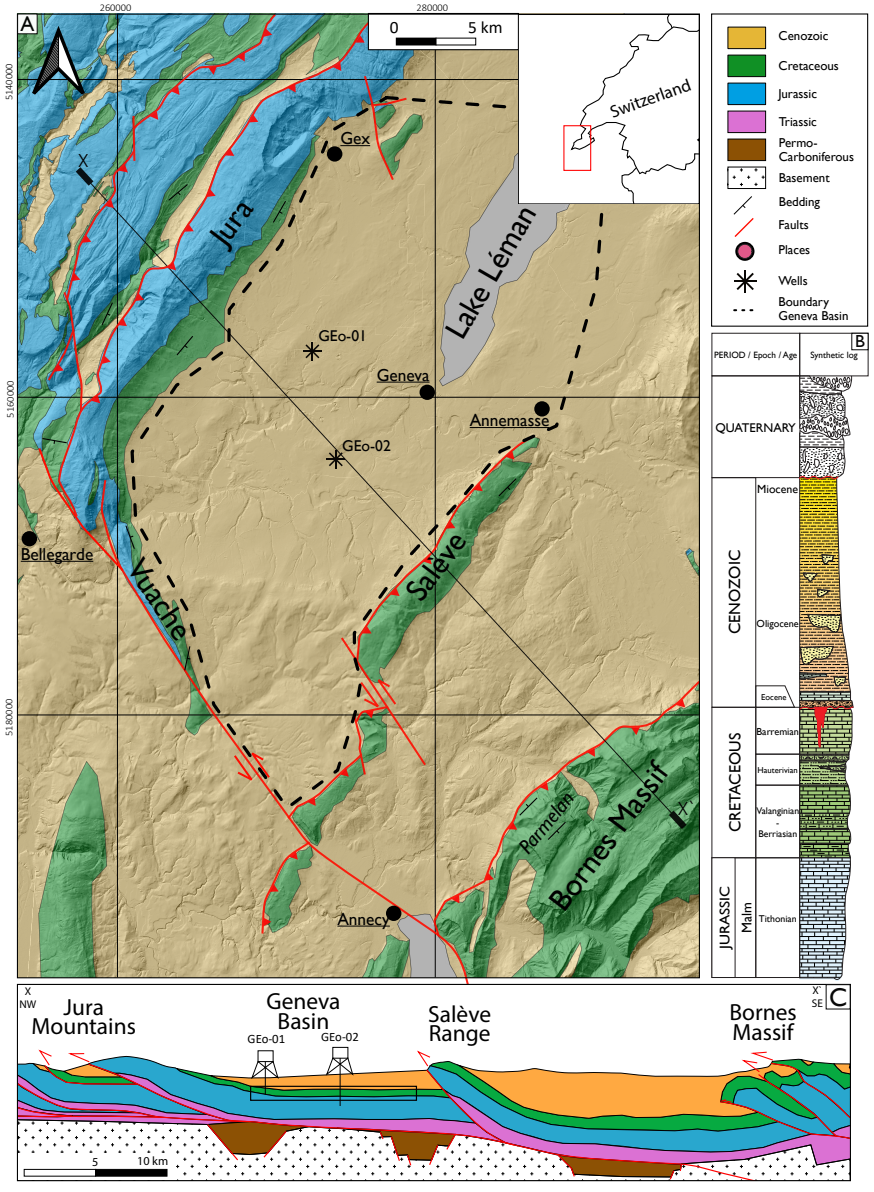

Figure 2. A) Simplified geological map modified after the 1:200.000 geological map of the Swiss Federal Office of Topography. The Geneva Basin (dashed black line) is located at the most western termination of the North Alpine Foreland Basin. Analogue outcrops of the Lower Cretaceous target reservoir are found in the Jura, Vuache, Salève and Bornes Massif (Parmelan) mountain ranges. Coordinates in UTM 32N reference frame. B) Synthetic log of the sedimentary succesion in the Geneva Basin, from the Upper Jurassic upwards, after Moscariello (2019). The Malm and the Lower Cretaceous are both potential geothermal reservoirs in the basin. In this study, we focus on the Lower Cretaceous. C) Cross section showing the NW-verging Alpine thrusts that separate the target reservoir (black box) from the analogue outcrops. Modified after Bellahsen et al. (2014); Moscariello (2019); Kalifi et al. (2021); Marro et al. (2023)

https://doi.org/10.5194/egusphere-2025-4175
Preprint. Discussion started: 12 September 2025

On a large scale, the plateau is dissected by two sets of fractures with similar orientation as the vein arrays (figure 4). They range in length from 100 to 3000 m. In the field, they appear as narrow bundles (<1 m) of smaller sub-vertical fractures. Dissolution along these fractures has created a karst system that is connected to an extensive cave system below the plateau (Lismonde, 1983; Masson, 1985). On the plateau, there are no offset markers that indicate horizontal displacement along these structures and no kinematic indicators are observed. At the northern edge of the plateau however, in front of the entrance to the Diau cave (see figure 10 for location), these fractures intersect a vertical cliff, and here bed-parallel slickensides on the fracture planes are preserved. The shear fractures form a conjugate pair, so their structural attitude is similar to the vein arrays on top of the plateau, and are thus grouped into PA2. The associated stress regime of PA2 is a strike-slip regime, with $\sigma 1$ oriented NW-SE. This is similar to PA1, with the only change being a permutation of $\sigma 2$ and $\sigma 3$. Therefore, PA1 and PA2 together are considered as part of one event.

The third association (PA3) is also made up of a conjugated pair of sub-vertical vein arrays and tectonic stylolites, but with different orientations than those of PA2 (figure 3C). The dextral vein arrays strike ∼080°-260° and the sinistral arrays strike ∼120°-300°, with the cement of the veins being grey-coloured. The length of the discontinuities range from cm to 10s of meters. The stylolites are bed-perpendicular and strike ∼170°-350°. The veins that form the arrays occasionally cross-cut and displace those of PA2 (figure 3D), and are therefore interpreted as being younger in age. The paleostress regime related to this association is strike-slip, with $\sigma 1$ oriented ∼W-E.

To investigate how representative the above described associations are for the total network present on the Parmelan, we measured augmented circular scanlines on 7 different pavements on the Parmelan (see figure4 for location). Up to 75% of the total discontinuities observed can be understood within the framework of the predefined associations, and the majority belong to PA3 5. The percentages vary per pavement investigated, illustrating the spatial variability of the background network.

4.2 Jura and Vuache

Four different associations have been documented in the Jura and Vuache. In all cases, they formed prior to tilting of the strata. The first association (JA1) comprises a conjugate pair of shear fractures with a low-angle with respect to the bedding and bed-perpendicular, tectonic stylolites (figure 6A). The strike of the shear fractures and stylolites is ∼035°-215°. Slickensides on the shear planes indicate reverse kinematics. The reconstructed $\sigma 1$ of JA1 is oriented NW-SE.

The second association (JA2) is made up of a conjugated pair of bed-perpendicular shear fractures (figure 6B), together with tectonic stylolites. Sinistral fractures strike ∼170°-350°, dextral fractures strike ∼110°-290°. Slickensides on the shear planes are always parallel the bedding. Tectonic stylolites strike of ∼035°-215°, similarly as those of JA1. The stress regime of JA2 is strike-slip, with $\sigma 1$ oriented NW-SE. The difference between JA1 and JA2 is a premutation of $\sigma 2$ and $\sigma 3$. Therefore, they are grouped into a single event.

The third association (JA3) is comprised of ∼000°-180° striking reverse shear fractures with a low angle with respect to the bedding (figure 6C), and bed-perpendicular tectonic stylolites. They formed in a reverse stress regime with $\sigma 1$ oriented W-E.

The fourth association (JA4)is expressed by bed-perpendicular ∼140°-320° striking sinistral shear fractures and ∼075°-255° striking dextral shear fractures (figure 6D), together with ∼010°-100° striking bed-perpendicular stylolites. This association is

https://doi.org/10.5194/egusphere-2025-4175
Preprint. Discussion started: 12 September 2025

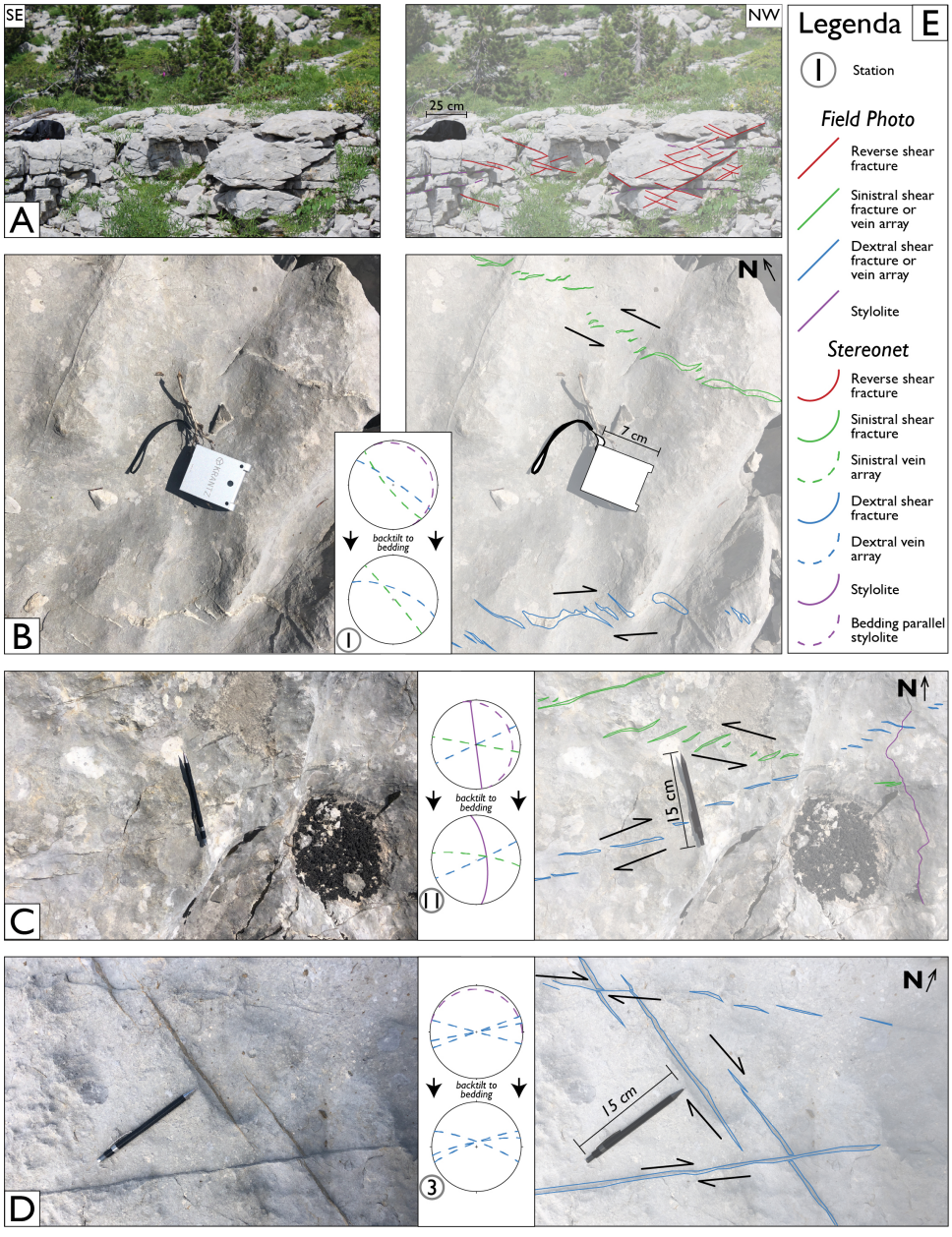

Figure 3. Field examples of DAs on the Parmelan. A) Low-angle conjugate pair of shear fractures (PA1) with minimal displacement. Dissolution along the shear planes make them clearly visible on bed-perpendicular exposures. B) Top view image of a conjugate pair of vein arrays of PA2. C) Top view image of PA3 conjugate pair of vein arrays in association with a bed-perpendicular stylolite. D) Dextral vein array of PA3 crosscuts and slightly displaces a dextral vein array of PA2, indicating the relative timing of formation of the two associations. All stereonets, here in and in following figures, are lower hemisphere projections. E) Legenda for the colours used on the intepretation of the photographs and stereonets.

https://doi.org/10.5194/egusphere-2025-4175
Preprint. Discussion started: 12 September 2025

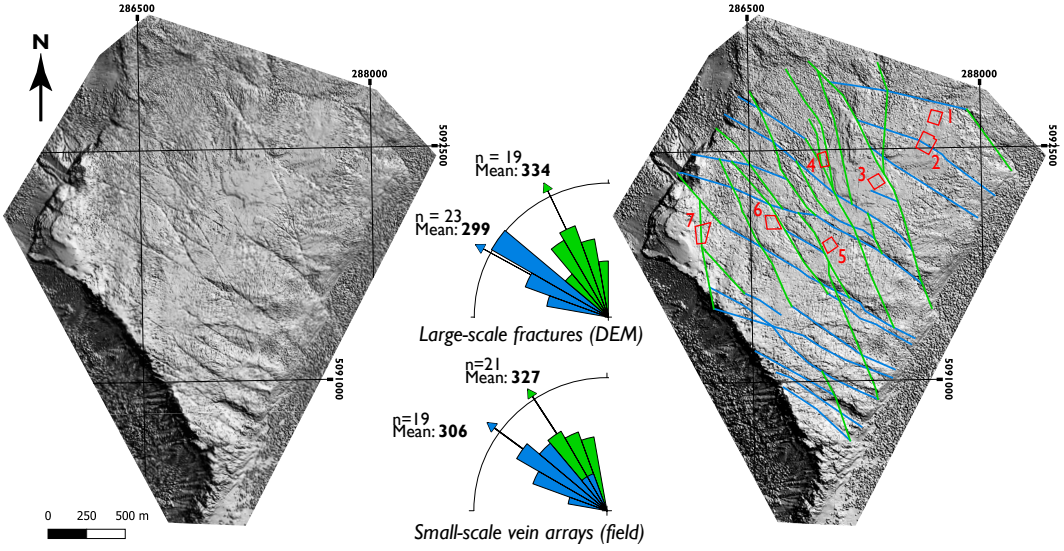

Figure 4. Digital elevation model of the Parmelan derived from LiDAR HD survey of IGN. The large-scale fracture network on the plateau is clearly visualized. The two main orientation of this network (upper rose diagram) correspond well with the orientations of the vein arrays of PA2 (lower rose diagram). At the northern plateau, opposing sense of shear is observed on these fractures, and therefore they are also grouped into PA2. The red insets refer to the pavements where circular scanlines are taken (see Table 1 for the results of the scanlines). Pavement 2 is shown as example in figure 5. For the colour code of the traced fractures, see legenda of figure 3E.

indicative of a strike-slip regime with $\sigma 1$ oriented W-E. This orientation is the same as JA3, and therefore they are part of the same event.

4.3 Salève

In the Salève, only one (SA1) is documented. Shear fractures that strike ∼030°-210° and have a low angle with respect to the bedding (figure 7) are associated together with ∼035°-215° striking bed-perpendicular stylolites. The related stress field is a reverse regime with $\sigma 1$ oriented NW-SE.

4.4 Regional discontinuity-forming events

Based on the orientation of $\sigma 1$ of the associations in the different studied areas, we can define two regional discontinuity formation events (figure 9). The first event (E1) is characterized by a NW-SE trending, sub-horizontal $\sigma 1$. This orientation of $\sigma 1$ is both recorded by the reverse associations (PA1, JA1 & SA1) as well as by strike-slip associations (PA2 & JA2). In all outcrops, the reverse regime is similarly expressed by low-angle conjugate pairs of shear fractures. Bed-perpendicular vein arrays of the strike-slip association are also observed in the Parmelan, Jura and Vuache. On top of this, in the Jura and Vuache, the strike-slip association is also expressed by conjugated brittle, sub-vertical shear fractures.

The second event (E2) is also made up of a reverse and strike-slip association, but with a sub-horizontal $\sigma 1$ oriented ∼W-E (figure9). In the Parmelan, only the strike-slip association is documented in the form of vein arrays and bed-perpendicular

https://doi.org/10.5194/egusphere-2025-4175
Preprint. Discussion started: 12 September 2025

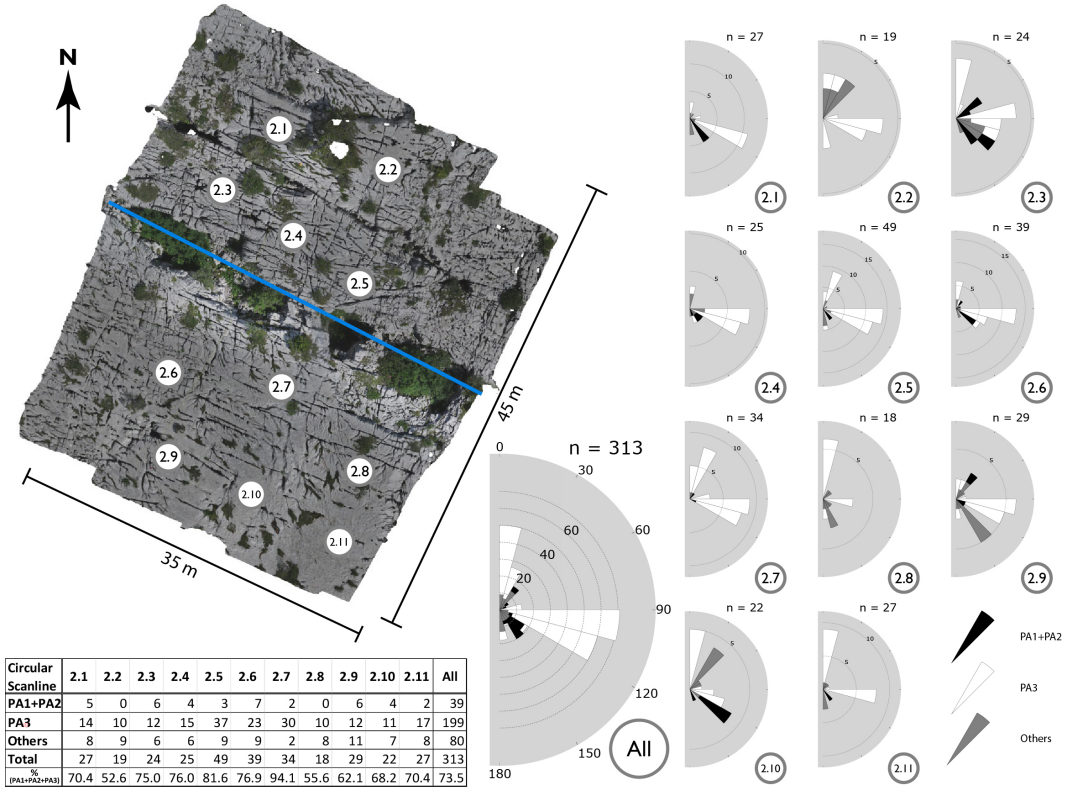

Circular Scanline	2.1	2.2	2.3	2.4	2.5	2.6	2.7	2.8	2.9	2.10	2.11	All
PA1+PA2	5	0	6	4	3	7	2	0	6	4	2	39
PA3	14	10	12	15	37	23	30	10	12	11	17	199
Others	8	9	6	6	9	9	2	8	11	7	8	80
Total	27	19	24	25	49	39	34	18	29	22	27	313
% (PA1+PA2+PA3)	70.4	52.6	75.0	76.0	81.6	76.9	94.1	55.6	62.1	68.2	70.4	73.5

Figure 5. UAV-derived orthorectified image of a pavement on the Parmelan (for location, see figure 4). Augmented circular scanlines with 1m radius show that the majority (75 %) of the observed discontinuities are in line with the qualitatively defined associations in station 4 (for location, see figure 10, for definition DAs, see figure 8). The scanlines are taken on both sides of a large-scale ENE-WSW fracture (blue line, see figure 4). There is no significant change in intensity of the discontinuities closer this fracture, suggesting that the large-scale fracture does not control the geometry of the total discontinuity network.

stylolites (PA3). In the Jura and Vuache, there is also a reverse association documented (JA3) with similar $\sigma 1$ as a strike-slip association (JA4). The latter is mainly depicted by bed-perpendicular shear fractures, and less so by vein arrays, in contrast to the Parmelan.

220 A pre-tilting relative timing for E1 and E2 is observed in all studied areas. This implies that E1 and E2 were formed prior to Alpine fold-and-thrusting, and thus form the background network. As these events are consistently observed on all sides of the Geneva Basin where the target reservoir is located, we predict the presence of this background network in the subsurface as well.

https://doi.org/10.5194/egusphere-2025-4175
Preprint. Discussion started: 12 September 2025

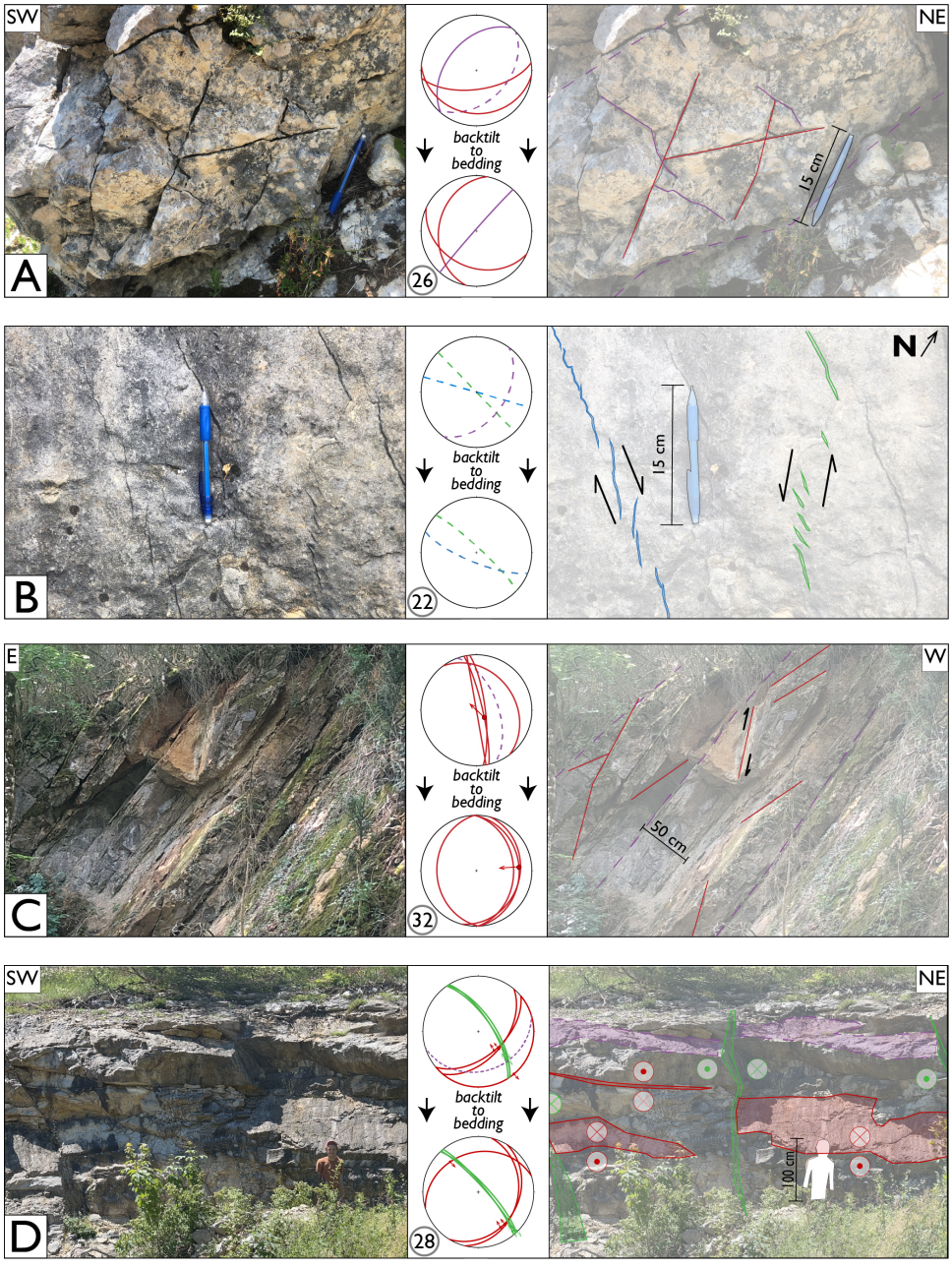

Figure 6. Field examples from the Jura. A Reverse shear fractures with low angle with respect to the bedding, in association with a bed-perpendicular stylolite together form the reverse association JA1. B Top view of a bedding surface displaying a conjugate pair of vein arrays. Together with similarly oriented bed-perpendicular shear fractures they form a strike-slip association JA2. C Tilted shear fractures at low angle with respect to the bedding. The strike after backtilting is ~N-S. They form the reverse association JA3. D Reverse fractures of JA1 are cross-cut by bed-perpendicular, sinistral shear fractures of JA4. The plunge of the slickensides on these shear fractures indicates they formed prior to tilting of the bedding. For legenda see figure 3E.

https://doi.org/10.5194/egusphere-2025-4175
Preprint. Discussion started: 12 September 2025

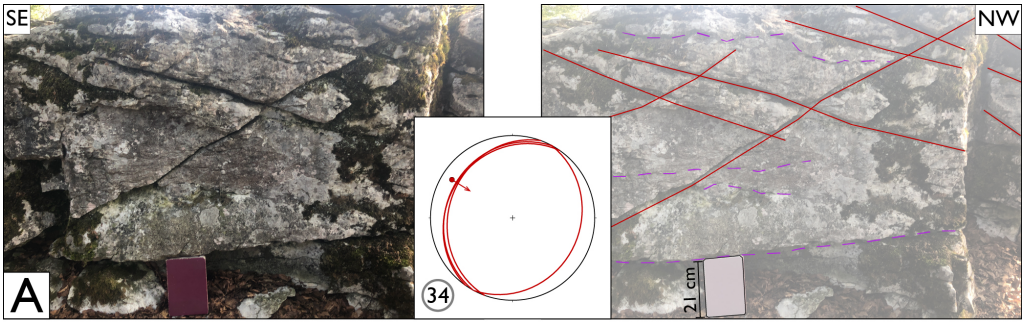

Figure 7. Field example from the Salève. A conjugate pair of reverse shear fractures at low angle with the bedding define the reverse association SA1. For legenda see figure 3E.

Table 1. Results of the augmented circular scanlines measured on the Parmelan. See figure 4 for the locations of the pavements. Results of circular scanlines of pavement 2 are illustrated in figure 5.

Pavement	No. of Scanlines (1m radius)	Total discontinuities	PA1 + PA2	PA3	Percentage of total
1	9	276	4	79	30.1%
2	11	313	39	191	73.5%
3	12	207	32	110	68.6%
4	6	85	8	39	55.3%
5	9	308	31	84	37.3%
6	4	150	5	79	56.0%
7	4	126	17	70	69.0%

5 Improving BHI interpretation

5.1 Description of GEo-01 and GEo-02

We use the prediction of the background network in the subsurface of the Geneva Basin based on the analogue outcrops for the interpretation of BHI of two geothermal wells drilled in the basin (GEo-01 and GEo-02, for location see figure 2). The discontinuities of which the orientation fits within the predicted background network are identified in the dataset and subsequently considered as part of the background network. Then, we evaluate the proportion of the background network with respect to all discontinuities observed in the well.

The two investigated wells both penetrate the Lower Cretaceous carbonates, and as there are no cores of the wells, all features are interpreted on the BHI only (Doesburg, 2023). In GEo-01, the Lower Cretaceous is observed between 411 m and 533 m (MD). In this well, two types of image logs are acquired for fracture analysis: optical borehole imaging (OBI) and acoustic borehole imaging (ABI). GEo-02 is located 7 km south-southeast of GEo-01 and here the Lower Cretaceous is found at a depth between 770 m to 996 m (MD). For this well, only ABI-logs are available.

https://doi.org/10.5194/egusphere-2025-4175
Preprint. Discussion started: 12 September 2025

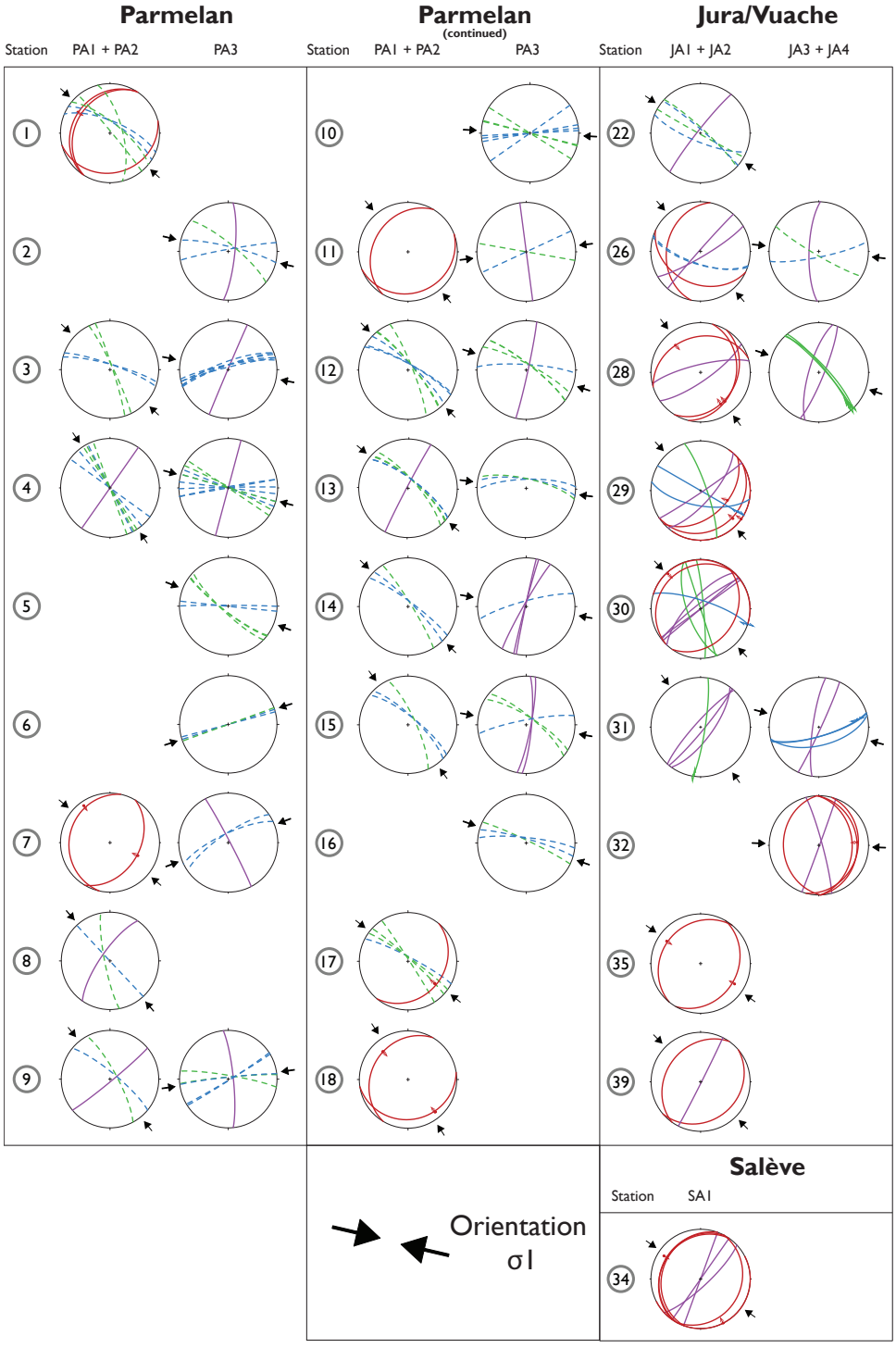

Figure 8. Stereonets of the events documented in all the stations of the analogue outcrops. All data is backtilted with respect to the bedding. The black and white arrows are the inferred orientations of $\sigma 1$ of E1 and E2 respectively, and correspond to the arrows plotted on figure 10. For the legenda of the colours, see figure 3

https://doi.org/10.5194/egusphere-2025-4175
Preprint. Discussion started: 12 September 2025

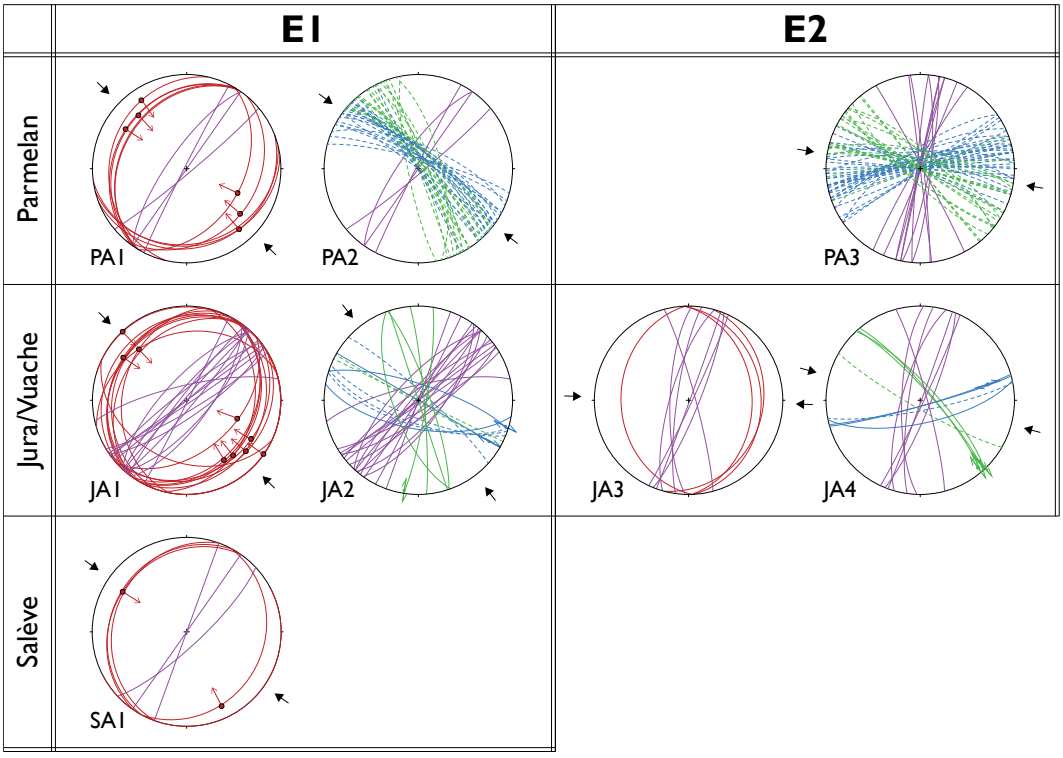

Figure 9. The associations of the different outcrops grouped into regional pre-tilting events, based on the orientation of $\sigma 1$. In all outcrops, a reverse association with $\sigma 1$ oriented ∼NW-SE is observed (PA1, JA1, SA1). In the Jura and Parmelan, a strike-slip association (PA2 and JA2) with similarly oriented $\sigma 1$ is documented, and together they are grouped into E1. E2 is predominantly a strike-slip association, complemented by a reverse association in the Jura/Vuache. E2 is not observed in the Salève, presumably due to a lack of exposures. All data is backtilted with respect to the bedding. For legenda see figure 3E.

The feature picks are divided over 5 different categories, following the methodology of Doesburg (2023); bedding, veins, open fractures, induced fractures and unclassified fractures. Bedding planes are defined by their repetitive character and the fact that they cannot cross-cut any other feature. Veins are highly reflective in OBI, whereas open fractures are transmissive. Veins are invisible on ABI and could therefore not be picked on the image logs of GEo-02. If feat are transmissive in OBI, have an irregular surface and the dip angle is high (>85 degrees) they are classified as induced fractures, although it should be noted that separating induced fractures from natural fractures remains a challenge (Lorenz and Cooper, 2017). Features that are both transmissive in OBI and have a low amplitude on the ABI are interpreted as open fractures. Distinguishing mode-I from mode-II is not possible on the image logs, so they are not differentiated during the picking of fractures. If a fracture pick did not meet any of the above criteria, it was not classified.

Firstly, the bedding planes are separated from the other interpreted features. In GEo-01, a total of 195 bedding surfaces are identified (figure 11). When plotted against depth, the dip direction of these planes exhibit a clockwise rotation with depth, from north-dipping at the top, gradually transitioning into south-dipping at the bottom. Also, the dip angle varies with depth, with a low angle at the top and bottom, but a gradual increase between 440-480 m (MD) up to 60°, giving an overall bell-shaped

https://doi.org/10.5194/egusphere-2025-4175
Preprint. Discussion started: 12 September 2025

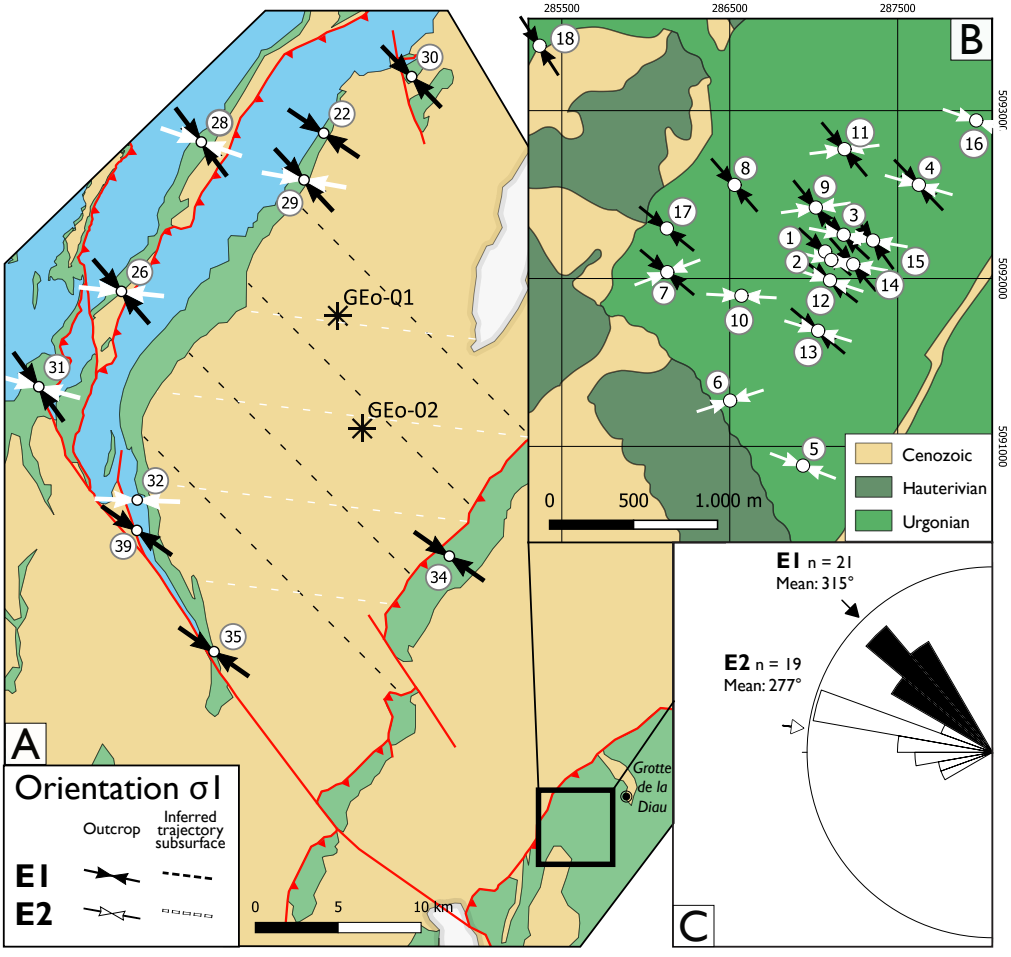

Figure 10. Overview of the mapped orientation of $\sigma 1$ of the regionally defined events E1 and E2 recorded in A) the Jura, Vuache, Salève and B) Parmelan C) Rose diagram of the orientations of $\sigma 1$ showing that there is a $\sim$45° anticlockwise rotation between E1 and E2.

curve. In GEo-02, a total of 176 bedding planes are picked (figure 11). In contrast to GEo-01, the dip direction remains constant with a dip towards the ESE and a dip angle between 10-20°.

For the implementation of the prediction based on outcrop work, we only considered the natural fractures (open fractures and veins), and discarded the induced and unclassified picks from the datasets. Then, the total amount of natural fractures observed in GEo-01 is 820, and for GEo-02 is 211. To compare these discontinuities with the outcrop prediction, they were backtilted with respect to the closest bedding measurement on the BHI (figure 12). The backtilted discontinuities are subsequently compared with the predicted background network as defined in the outcrops.

https://doi.org/10.5194/egusphere-2025-4175
Preprint. Discussion started: 12 September 2025

5.2 Comparison with DAs observed in the field

The orientations of the regional events in the outcrop are used to predict the geometry of individual discontinuity sets that make the background network in the subsurface. We consider the average orientation of the principal stresses of the regional events, and define orientations of discontinuity sets related to this orientation. For E1, the orientation of $\sigma 1$ is 135-315° and for E2 it is 097-277° (figure10). For the low angle shear fractures, we assumed a strike perpendicular to $\sigma 1$ with a dip angle of 30 degrees. For the stylolites, the strike is also perpendicular to $\sigma 1$, but with a dip angle of 90 degrees (perpendicular to the bedding). As in the outcrop, the majority of the discontinuities that make up the strike-slip associations are bed-perpendicular vein arrays, we considered a 15 degree angle between $\sigma 1$ and the strike of the vein arrays for the prediction in the well. Lastly, the opening fractures are bed-perpendicular with a strike parallel to $\sigma 1$. The combination of these sets are used to identify the fractures in the well that fit within this predicted assoications. If a fracture pick on the BHI deviates less than 30° (azimuth + dip) from the predicted orientation of a set, these fractures are considered as part of that discontinuity set (figure 12).

For the well GEo-01, 350 discontinuities (44% of total) fit in the associations of E1 and E2, of which 236 are open fractures, and 114 veins. In GEo-02, the total number of discontinuities that fit the predicted associations is 104 (50% of total). As there is no ABI for Geo-02, all the fractures that are identified are open. The contribution of E1 and E2 is about equal. The majority of the discontinuities in the two wells are low-angle shear fractures (175 and 86 for Geo-01 and Geo-02 respectively).

6 Discussion

6.1 The robustness of DAs as the analog link

The regional events captured by the method of DAs reveal similar paleostress orientations as previous studies focusing on the deformation history of the Parmelan (Berio et al., 2021) and the Jura and Vuache ranges (Homberg et al., 1999, 2002). In the Parmelan, Berio et al. (2021) define two pre-folding events with a reverse and strike-slip component with an ∼NW-SE orientation of $\sigma 1$, similar to E1. These authors also document a strike-slip event with an ∼E-W oriented $\sigma 1$ identical to E2 but interpret this event to be post-folding (Berio et al., 2021). In the Jura and Vuache ranges, the reverse and strike-slip regimes of E1 are also observed by Homberg et al. (1999). However, the inferred timing of these regimes is different; only the strike-slip component is interpreted as pre-tilting of the strata, whereas the reverse regime is considered syntectonic, because the majority of the observed reverse slip vectors were not pre-folding (Homberg et al., 2002). This is in contrast to our observations of clearly pre-folding shear fractures (fig. 6A).

The main difference between the DA method and previous studies is the interpreted timing of discontinuity-forming events, which reflects the specific aim of the methodology proposed in this study. The goal of the DA method is to use the outcrop as an analogue of the subsurface to better predict the geometry and flow efficiency of the fracture network present at depth that is not directly observable. On the contrary, the studies of Berio et al. (2022) and Homberg et al. (2002) focus on the deformation history of the outcrop itself, aiming at retracing the chronological succession of events that created the discontinuities in the outcrop. The consequences of these different approaches are best illustrated with the reverse regime of E1. If this event is linked

https://doi.org/10.5194/egusphere-2025-4175
Preprint. Discussion started: 12 September 2025

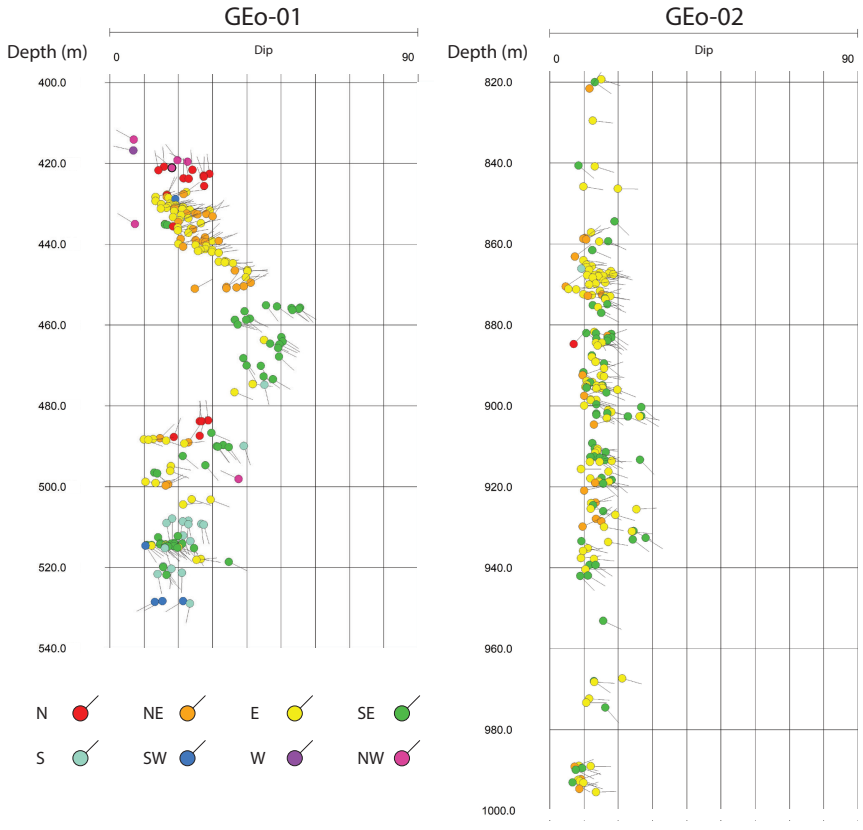

Figure 11. Tadpoles of bedding picks versus depth on GEo-01 and GEo-02 after Doesburg (2023). In GEo-01, there is a variation in both azimuth and dip with depth. The bell-shaped curve suggests the presence of a fold, potentially related to a fault around 480 m depth. This contrasts with GEo-02, where no change is observed in bedding orientation with depth.

to folding, it may be expected to produce localized deformations, opposed to the distribution of a background network (Watkins et al., 2015b). However, this event, producing reverse shear fractures, could also be interpreted as having formed during the layer parallel shortening (LPS) phase before the onset of regional folding. Lacombe et al. (2021) dated the sequence of events shaping a series of folds observed in the Apennines, Pyrenees and in the Rocky Mountains. They found that the LPS-phase largely predates the onset of localized deformations occurring during fold tightening. Therefore, the LPS deformation phase is likely to produce the same diffuse fractures observed in the Vuache and the Jura. Considering the E1 regime as localized and restricted to fold structures dramatically changes the prediction of these features in the subsurface. In the absence of folds in the subsurface, these fractures will be overlooked, although they are largely present in the investigated wells in the Geneva basin (see fig12).

In the case of E2, the key aspect of the DA-method is that it targets regional events to enhance the predictability of the method. On the Parmelan itself, there is no direct evidence for the relative timing of E2 with respect to the folding. In the

https://doi.org/10.5194/egusphere-2025-4175
Preprint. Discussion started: 12 September 2025

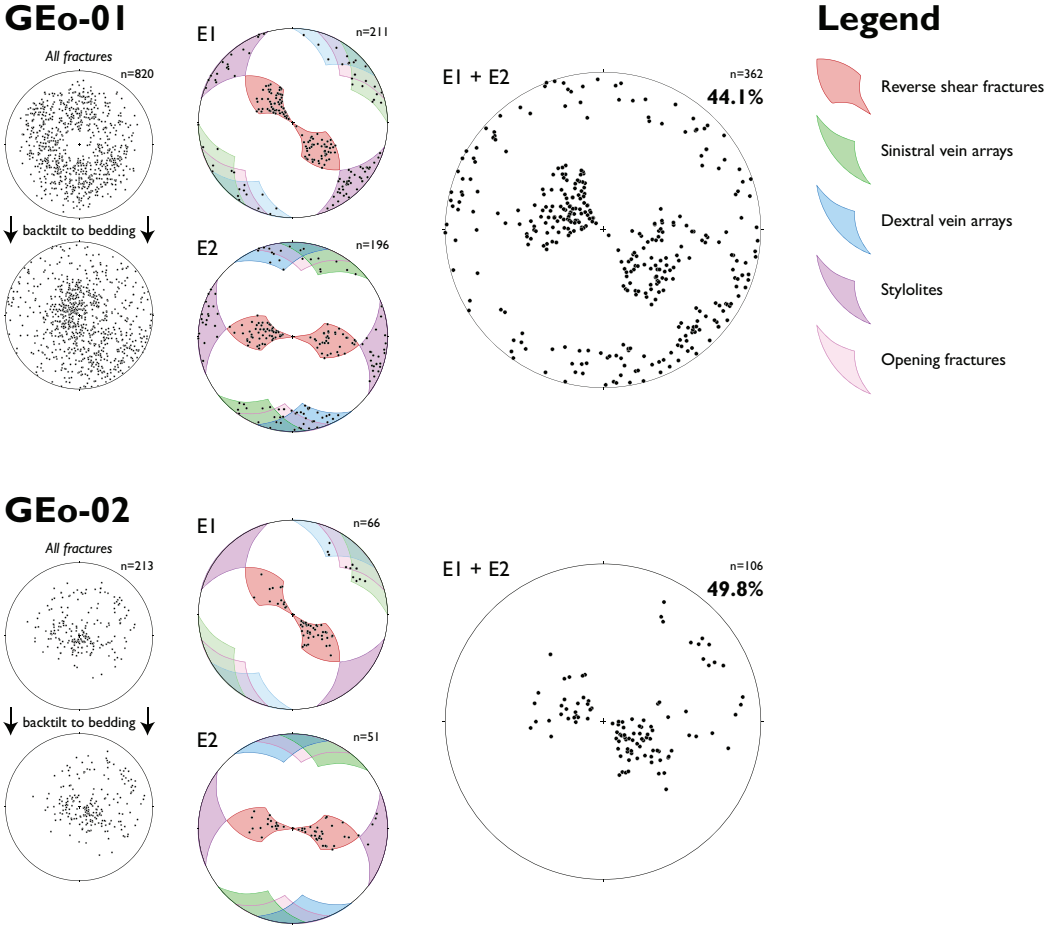

Figure 12. All fractures interpreted from the BHI of GEo-01 and GEo-02 by Doesburg (2023) compared with the predicted associations based on the outcrops. First, the fractures in the well are backtilted with respect to the bedding, as the predicted associations are formed pre-tilting. Then, the fractures that fit in the predicted associations of E1 and E2 are counted. The coloured areas are based on the average orientations of $\sigma 1$ of the two regional events (figure 10C), with a deviation margin of 30° (azimuth + dip). There is a small overlap between some sets of E1 and E2: fractures are not counted double when calculating the total percentage of the predicted fractures.

https://doi.org/10.5194/egusphere-2025-4175
Preprint. Discussion started: 12 September 2025

Jura however, shear fractures of E2 are consistently tilted with the bedding (e.g., figure 6C) and thus formed prior to tilting. Therefore, we interpret E2 as part of the background network and consequently present in the subsurface. Absolute dating of the calcite veins that are part of the background network could potentially resolve the issue of the timing, but so far, geochronology studies in the region have only focused on dating fault activity (Smeraglia et al., 2021; Looser et al., 2021).

6.2 DAs as the guideline for BHI interpretations

Boreholes are the only way to sample and characterise the sub-seismic scale discontinuity network in the subsurface of the Geneva Basin. Many data collection methods of faults and fractures are prone to subjective bias, both in the subsurface (Bond et al., 2007) and in outcrops (Andrews et al., 2019; Peacock et al., 2019). However, the influence of bias on BHI interpretations has rarely been investigated (Zarian and N. Dymmock, 2010). The reproducibility of BHI interpretation remains a major challenge, leading to discrepancies in fracture frequency analysis and inconsistent fracture orientation among different interpreters. These uncertainties have a large impact on the characterization of the fracture network and the population of fracture models of the reservoir. For instance, Tutuarima et al. (2023) studied the BHI of a deep exploration well targeting the geothermal Triassic sandstone reservoirs in the West Netherlands Basin. Over 900 fractures picked; these authors identified that only 32 % of them are natural. Before this work, two consultancy companies studied the same interval, picked roughly the same number of features, and interpreted either 100% or as low as 2.8% as being natural fractures. This discrepancy has large implications for whether considering the targeted reservoir as naturally fractured and therefore suitable for geothermal resource exploitation.

To reduce biases in fracture interpretation, Andrews et al. (2019) propose to develop a clear sampling strategy before the actual interpretation. The robust analogy between outcrops and the subsurface provided by the DA method presented in this paper has the potential to create such a strategy for BHI interpretations and, in this way, reduce the impact of bias. The two events that shape the predicted background network in the subsurface of the Geneva Basin are composed of discontinuity sets with a known range of orientations. An adequate fracture picking strategy in the BHI could be to temporarily discard all features that fall significantly outside this predefined range. The resulting picking will therefore focus on isolating the background network from more recent structural objects. After this, the impact of the background network on the flow behaviour of the reservoir can be assessed (see Sect. 6.3).

DAs also improve BHI interpretation by predicting the discontinuity type of identified features. Genter et al. (1997) and Fernández-Ibáñez et al. (2018) integrated cores with image logs to improve the subsurface fracture characterization. Both studies show that the correlation with the core is essential for assigning the type of discontinuity to the BHI interpretation. However, cores are expensive to drill, and therefore, often only BHIs are available for subsurface fracture characterization. The discontinuity sets defined on the BHI are then all considered as barren or Mode-I fractures. Based on this assumption, a classical workflow consists of defining fracture sets, extracting statistical distributions for these sets, and stochastically extrapolating these distributions at the reservoir scale in a discrete fracture network model (Hosseinzadeh et al., 2023).

However, the type of discontinuity will impact the evaluation of the flow behaviour of the network in different ways. Bruna et al. (2019) demonstrated that stylolites can be either flow conductive or form flow barriers and could potentially induce compartmentalisation in subsurface reservoirs. Hooker et al. (2012) and Lander and Laubach (2015) showed that Mode-I

https://doi.org/10.5194/egusphere-2025-4175
Preprint. Discussion started: 12 September 2025

fractures are good flow conductors if cement bridges create a natural propping mechanism in the fracture. Finally, Bisdom et al. (2016) emphasised that the roughness of a fracture has an impact on its capacity to be reactivated under present-day stress field, which in turn influences its hydraulic aperture under reservoir conditions. These authors also add that typically, Mode-II fractures have a higher roughness than Mode-I fractures, therefore highlighting the importance of being able to constrain fracture type at depth. The DA-methodology provides a prediction of the discontinuity type in the borehole, even when the resolution of the BHI is too low to determine this. This information can be considered during fracture modeling and subsequent flow simulations.

6.3 Impact on fracture modeling and geothermal exploration

Isolating the background network from the total network will improve fracture modeling because the structural driving mechanism that shapes the background network is fundamentally different than other parts of the total network. Maerten et al. (2016) developed a method that links discontinuities observed in the well with seismic-scale faults. A given number of random far-field stress states are simulated around the faults, and the perturbation of the stress directions around the faults is calculated. For each simulated stress state, the number of small-scale discontinuities whose orientation fits within the modeled stress field is counted (goodness of fit). The stress state with the highest number of fitting discontinuities is considered the best stress regime, and the discontinuities falling outside this model are discarded from the dataset. The input data for these models are generally all the fractures interpreted from wells. If the background network is not isolated from fractures related to more localized deformations (e.g., faults), the goodness of fit will be affected by the very different mechanisms that these contrasted fracture populations experienced.

Besides integrating more geology into the process of modeling fracture networks, the DA method has implications for upscaling. Berre et al. (2019) advocated for mixing explicit and implicit representation of fractures in the model as an effective up-scaling method to balance the accuracy of up-scaling whilst preserving the geometrical complexity. Typically, the selection criterion between implicit and explicit representation is the length of the fractures (Lee et al., 2001). In addition to this method, we propose to use the genetic origin of the fracture as a second criterion. The background network is very suitable for up-scaling strategies, due to its regional character, in contrast to the discontinuities formed by local drivers. Here, we will investigate when it is possible to up-scale the background network as a matrix property on the reservoir scale.

The first step is to evaluate the importance of the background network on the effective permeability k_{eff} of the reservoir. Numerical work has suggested that there is a relationship between fracture density P_{21} and effective permeability k_{eff} of a fractured medium (Agbaje et al., 2023), so a first-order approximation is to consider the fracture density P_{21} of the background network. The density can be derived from either the outcrop using scanlines (fig 5) or from the well (fig 12). Agbaje et al. (2023) showed that the coupled fracture density and k_{eff} display distinct behaviours related to the degree of connectivity and the degree of saturation of the networks. If the P_{21} is below a certain threshold value, the fractures are not connected and will not contribute to k_{eff}. This implies that the background network has no significant impact on fluid flow, and can thus be discarded on the scale of the reservoir. On the other hand, if the P_{21} is above a certain value, all fractures of the background network are practically connected, and adding more fractures to the network does not affect k_{eff}. This is the percolation

https://doi.org/10.5194/egusphere-2025-4175
Preprint. Discussion started: 12 September 2025

threshold. As a consequence, the background network can be up-scaled as a matrix property on the reservoir scale, with a permeability of k_{eff}. It should be noted that the two threshold values in the curve depend on the statistics of the lengths of the fractures in the network (maximum and minimum length, and length distribution). The critical fracture density is between these two extremes, where small changes in density have a large effect on k_{eff}. In these cases, it is not possible to up-scale the background network directly, and explicit representation of the discontinuities is needed. This can be done with DFN-solvers based on statistical parameters (Kamel Targhi et al., 2024).

At the same time, the analysis of the BHI has shown that not all discontinuities observed in the well can be placed in the framework of the background network. These discontinuities are thus likely created by local drivers and scale differently on the reservoir scale than the background network. As the background-related discontinuities are isolated from the dataset, the earlier discussed method of Maerten et al. (2016) is a suitable approach to model the remaining part of the discontinuities.

This dynamic workflow will de-risk future geothermal drilling projects in different ways. The separate modeling of the permeability of the background network can be used to assess whether the background only can already produce economically viable fluid volumes, or if seismic-scale discontinuities are essential for production. Also, the well-placing strategy can be adjusted to the heterogeneity of the background permeability field. For example, in the Geneva Basin, most of the background discontinuities are striking NE-SW, and thus, a higher permeability in that direction is expected. A deviation of the well perpendicular to this strike will therefore optimize the well screen and thus the fluid inflow.

7 Conclusions

In this study, we presented a novel approach to connect outcrop studies of discontinuities with subsurface characterization of discontinuity networks. Associations of genetically related discontinuities that form the background network produced by the far-field stress are defined in the field. The regional character of the background network provides a robust link between analogue outcrops and subsurface target reservoirs. This link is used to improve interpretations of borehole images. By applying this methodology to analogue outcrops of a naturally fractured geothermal reservoir in the Geneva Basin, we have shown that:

1. DAs are robust paleostress indicators that enable the reconstruction of the paleo stress field in which the background discontinuity network is formed
2. The regional character of the background network makes it a robust link between the outcrop and the subsurface
3. Analogue outcrops of the Lower Cretaceous carbonates in the Geneva Basin reveal two regional discontinuity-forming events that occurred before Alpine fold-and-thrusting
4. 40-50% of discontinuities observed on BHI from the target reservoir can be explained by the regional events constrained by the work done on analogue outcrops
5. Outcrop study is a time and cost-efficient method to obtain a first-order evaluation of the contribution of the background network in the subsurface.

https://doi.org/10.5194/egusphere-2025-4175
Preprint. Discussion started: 12 September 2025

Data availability. The measurements displayed in the stereonets of figure 8 are provided as a supplementary dataset.

Author contributions. JH: Writing - original draft preparation, Conceptualization, Methodology, Investigation, Data Curation, Visualization; POB: Conceptualization, Supervision, Writing - review and editing; GB: Conceptualization, Supervision, Writing - review and editing; MD: Formal Analysis; AM: Supervision, Writing - review and editing

Competing interests. The authors declare that they have no conflict of interest.

Acknowledgements. We would like to thank the Service Industriel de Geneve for making the BHI-data of the two wells in the Geneva Basin available to us. The first author is grateful for the Molengraaf Fonds for providing financial support for the conducted fieldwork. The assistance of Nil Feliu during the collection of the circular scanline data is highly appreciated. Didier Rigal and Jean-Marc Verdet are kindly thanked for sharing their endless knowledge on the Parmelan cave system, and for their guidance during the excursion in the Grotte de la Diau.

https://doi.org/10.5194/egusphere-2025-4175
Preprint. Discussion started: 12 September 2025

References

Agbaje, T. Q., Ghanbarian, B., and Hyman, J. D.: Effective Permeability in Fractured Reservoirs: Discrete Fracture Matrix Simulations and Percolation-Based Effective-Medium Approximation, Water Resources Research, 59, e2023WR036505, https://doi.org/10.1029/2023WR036505, 2023.

Anderson, E.: The Dynamics of Faulting, Transactions of the Edinburgh Geological Society, 8, 387–402, https://doi.org/10.1144/transed.8.3.387, 1905.

Andrews, B. J., Roberts, J. J., Shipton, Z. K., Bigi, S., Tartarello, M. C., and Johnson, G.: How do we see fractures? Quantifying subjective bias in fracture data collection, Solid Earth, 10, 487–516, https://doi.org/10.5194/se-10-487-2019, 2019.

Angelier, J.: Inversion of Field Data in Fault Tectonics to Obtain the Regional Stress-III. A New Rapid Direct Inversion Method by Analytical Means, Geophysical Journal International, 103, 363–376, https://doi.org/10.1111/j.1365-246X.1990.tb01777.x, 1990.

Atkinson, G. M., Eaton, D. W., and Igonin, N.: Developments in understanding seismicity triggered by hydraulic fracturing, Nature Reviews Earth & Environment, 1, 264–277, https://doi.org/10.1038/s43017-020-0049-7, 2020.

Beach, A.: The Geometry of En-Echelon Vein Arrays, Tectonophysics, 28, 245–263, https://doi.org/10.1016/0040-1951(75)90040-2, 1975.

Bellahsen, N., Mouthereau, F., Boutoux, A., Bellanger, M., Lacombe, O., Jolivet, L., and Rolland, Y.: Collision Kinematics in the Western External Alps: Kinematics of the Alpine Collision, Tectonics, 33, 1055–1088, https://doi.org/10.1002/2013TC003453, 2014.

Berio, L. R., Storti, F., Balsamo, F., Mittempergher, S., Bistacchi, A., and Meda, M.: Structural Evolution of the Parmelan Anticline (Bornes Massif, France): Recording the Role of Structural Inheritance and Stress Field Changes on the Finite Deformation Pattern, Tectonics, 40, e2021TC006913, https://doi.org/10.1029/2021TC006913, 2021.

Berio, L. R., Mittempergher, S., Storti, F., Bernasconi, S. M., Cipriani, A., Lugli, F., and Balsamo, F.: Open–Closed–Open Palaeofluid System Conditions Recorded in the Tectonic Vein Networks of the Parmelan Anticline (Bornes Massif, France), Journal of the Geological Society, 179, jgs2021–117, https://doi.org/10.1144/jgs2021-117, 2022.

Berre, I., Doster, F., and Keilegavlen, E.: Flow in Fractured Porous Media: A Review of Conceptual Models and Discretization Approaches, Transport in Porous Media, 130, 215–236, https://doi.org/10.1007/s11242-018-1171-6, 2019.

Bertotti, G., De Graaf, S., Bisdom, K., Oskam, B., B. Vonhof, H., H. R. Bezerra, F., J. G. Reijmer, J., and L. Cazarin, C.: Fracturing and Fluid-flow during Post-rift Subsidence in Carbonates of the Jandaíra Formation, Potiguar Basin, NE Brazil, Basin Research, 29, 836–853, https://doi.org/10.1111/bre.12246, 2017.

Bisdom, K., Bertotti, G., and Nick, H. M.: A Geometrically Based Method for Predicting Stress-Induced Fracture Aperture and Flow in Discrete Fracture Networks, AAPG Bulletin, 100, 1075–1097, https://doi.org/10.1306/02111615127, 2016.

Bond, C., Gibbs, A., Shipton, Z., and Jones, S.: What do you think this is? "Conceptual uncertainty" in geoscience interpretation, GSA Today, 17, 4, https://doi.org/10.1130/GSAT01711A.1, 2007.

Brentini, M.: Impact d'une donnée géologique hétérogène dans la gestion des géo-ressources: analyse intégrée et valorisation de la stratigraphie à travers le bassin genevois (Suisse, France), Ph.D. thesis, Université de Genève, https://doi.org/10.13097/ARCHIVE-OUVERTE/UNIGE:103409, 2018.

Bruna, P.-O., Lavenu, A. P., Matonti, C., and Bertotti, G.: Are stylolites fluid-flow efficient features?, Journal of Structural Geology, 125, 270–277, https://doi.org/10.1016/j.jsg.2018.05.018, 2019.

Butler, R. W. H.: Hydrocarbon Maturation, Migration and Tectonic Loading in the Western Alpine Foreland Thrust Belt, Geological Society, London, Special Publications, 59, 227–244, https://doi.org/10.1144/GSL.SP.1991.059.01.15, 1991.

https://doi.org/10.5194/egusphere-2025-4175
Preprint. Discussion started: 12 September 2025

Cederbom, C. E., Sinclair, H. D., Schlunegger, F., and Rahn, M. K.: Climate-Induced Rebound and Exhumation of the European Alps, Geology, 32, 709, https://doi.org/10.1130/G20491.1, 2004.

Charollais, J., Mastrangelo, B., Strasser, A., Piuz, A., Granier, B., Monteil, E., Ruchat, C., and Savoy, L.: Lithostratigraphie, biostratigraphie, cartographie et géologie structurale du Mont Salève, entre l'Arve et les Usses (Haute Savoie, France), Revue de Paleobiologie, 42, 1–127, https://doi.org/10.5281/ZENODO.7446048, 2023.

Clavel, B., Charollais, J., Conrad, M., Du Chêne, R. J., Busnardo, R., Gardin, S., Erba, E., Schroeder, R., Cherchi, A., Decrouez, D., Granier, B., Sauvagnat, J., and Weidmann, M.: Dating and Progradation of the Urgonian Limestone from the Swiss Jura to South-East France, Zeitschrift der Deutschen Gesellschaft für Geowissenschaften, 158, 1025–1062, https://doi.org/10.1127/1860-1804/2007/0158-1025, 2007.

Clavel, B., Conrad, M. A., Busnardo, R., Charollais, J., and Granier, B.: Mapping the Rise and Demise of Urgonian Platforms (Late Hauterivian - Early Aptian) in Southeastern France and the Swiss Jura, Cretaceous Research, 39, 29–46, https://doi.org/10.1016/j.cretres.2012.02.009, 2013.

Clerc, N. and Moscariello, A.: A Revised Structural Framework for the Geneva Basin and the Neighboring France Region as Revealed from 2D Seismic Data: Implications for Geothermal Exploration, Swiss Bulletin für angewandte Geologie, 2020.

Deville, E. and Sassi, W.: Contrasting Thermal Evolution of Thrust Systems: An Analytical and Modeling Approach in the Front of the Western Alps, AAPG Bulletin, 90, 887–907, https://doi.org/10.1306/01090605046, 2006.

Doesburg, M.: Uncertainty Reduction in Image Log Fracture Interpretation, and Its Implications to the Geological History of the Geneva Basin, Switzerland, Master's thesis, TU Delft, Delft, https://resolver.tudelft.nl/uuid:a16d4d2b-d373-48a7-9e5c-b6f22d3045d0, 2023.

Fadel, M., Meneses Rioseco, E., Bruna, P.-O., and Moeck, I.: Pressure transient analysis to investigate a coupled fracture corridor and a fault damage zone causing an early thermal breakthrough in the North Alpine Foreland Basin, Geoenergy Science and Engineering, 229, 212 072, https://doi.org/10.1016/j.geoen.2023.212072, 2023.

Fernández-Ibáñez, F., DeGraff, J., and Ibrayev, F.: Integrating borehole image logs with core: A method to enhance subsurface fracture characterization, AAPG Bulletin, 102, 1067–1090, https://doi.org/10.1306/0726171609317002, 2018.

Genter, A., Castaing, C., Dezayes, C., Tenzer, H., Traineau, H., and Villemin, T.: Comparative analysis of direct (core) and indirect (borehole imaging tools) collection of fracture data in the Hot Dry Rock Soultz reservoir (France), Journal of Geophysical Research: Solid Earth, 102, 15 419–15 431, https://doi.org/10.1029/97JB00626, 1997.

Guglielmetti, L. and Moscariello, A.: On the Use of Gravity Data in Delineating Geologic Features of Interest for Geothermal Exploration in the Geneva Basin (Switzerland): Prospects and Limitations, Swiss Journal of Geosciences, 114, 15, https://doi.org/10.1186/s00015-021-00392-8, 2021.

Guglielmetti, L., Poletto, F., Corubolo, P., Bitri, A., Dezayes, C., Farina, B., Martin, F., Meneghini, F., Moscariello, A., Nawratil De Bono, C., and Schleifer, A.: Results of a Walk-above Vertical Seismic Profiling Survey Acquired at the Thônex-01 Geothermal Well (Switzerland) to Delineate Fractured Carbonate Formations for Geothermal Development, Geophysical Prospecting, 68, 1139–1153, https://doi.org/10.1111/1365-2478.12912, 2020.

Guglielmetti, L., Houlié, N., de Bono, C. N., Martin, F., Coudroit, J., Oerlemans, P., and Cremer, H.: HEATSTORE D5.2: Monitoring Results for the Geneva HT-ATES Case-Study, HEATSTORE project report, 2021.

Hancock, P.: Brittle Microtectonics: Principles and Practice, Journal of Structural Geology, 7, 437–457, https://doi.org/10.1016/0191-8141(85)90048-3, 1985.

https://doi.org/10.5194/egusphere-2025-4175
Preprint. Discussion started: 12 September 2025

Homberg, C., Lacombe, O., Angelier, J., and Bergerat, F.: New Constraints for Indentation Mechanisms in Arcuate Belts from the Jura Mountains, France, Geology, 27, 827, https://doi.org/10.1130/0091-7613(1999)027<0827:NCFIMI>2.3.CO;2, 1999.

Homberg, C., Bergerat, F., Philippe, Y., Lacombe, O., and Angelier, J.: Structural Inheritance and Cenozoic Stress Fields in the Jura Fold-and-Thrust Belt (France), Tectonophysics, 357, 137–158, https://doi.org/10.1016/S0040-1951(02)00366-9, 2002.

Hooker, J. N., Gomez, L. A., Laubach, S. E., Gale, J. F. W., and Marrett, R.: Effects of diagenesis (cement precipitation) during fracture opening on fracture aperture-size scaling in carbonate rocks, Geological Society, London, Special Publications, 370, 187–206, https://doi.org/10.1144/SP370.9, 2012.

Hosseinzadeh, S., Kadkhodaie, A., Wood, D. A., Rezaee, R., and Kadkhodaie, R.: Discrete fracture modeling by integrating image logs, seismic attributes, and production data: a case study from Ilam and Sarvak Formations, Danan Oilfield, southwest of Iran, Journal of Petroleum Exploration and Production Technology, 13, 1053–1083, https://doi.org/10.1007/s13202-022-01586-y, 2023.

Jenny, J., Burri, J., Mural, R., Pugin, A., Schegg, R., and Ugemach, P.: Le Forage Geothermique de Thonex-01 (Canton de Geneve): Aspects Stratigraphiques, Tectoniques, Diagenetiques, Geophysiques et Hydrogeologiques, Eclogae Geologicae Helvetiae, 88, 265–396, 1995.

Kalifi, A., Leloup, P. H., Sorrel, P., Galy, A., Demory, F., Spina, V., Huet, B., Quillévéré, F., Ricciardi, F., Michoux, D., Lecacheur, K., Grime, R., Pittet, B., and Rubino, J.-L.: Chronology of Thrust Propagation from an Updated Tectono-Sedimentary Framework of the Miocene Molasse (Western Alps), Solid Earth, 12, 2735–2771, https://doi.org/10.5194/se-12-2735-2021, 2021.

Kamel Targhi, E., Bruna, P.-O., Daniilidis, A., Rongier, G., and Geiger, S.: GeoDFN - A Flexible, Open-Source Software for Generating Geologically Consistent Discrete Fracture Networks, https://doi.org/10.4121/0DC9C47A-2294-4811-A0FE-E049CB15FF3D.V1, 2024.

La Bruna, V., Lamarche, J., Agosta, F., Rustichelli, A., Giuffrida, A., Salardon, R., and Marié, L.: Structural diagenesis of shallow platform carbonates: Role of early embrittlement on fracture setting and distribution, case study of Monte Alpi (Southern Apennines, Italy), Journal of Structural Geology, 131, 103 940, https://doi.org/10.1016/j.jsg.2019.103940, 2020.

La Bruna, V., Bezerra, F. H., Souza, V. H., Maia, R. P., Auler, A. S., Araujo, R. E., Cazarin, C. L., Rodrigues, M. A., Vieira, L. C., and Sousa, M. O.: High-permeability zones in folded and faulted silicified carbonate rocks – Implications for karstified carbonate reservoirs, Marine and Petroleum Geology, 128, 105 046, https://doi.org/10.1016/j.marpetgeo.2021.105046, 2021.

Lacombe, O., Beaudoin, N. E., Hoareau, G., Labeur, A., Pecheyran, C., and Callot, J.-P.: Dating folding beyond folding, from layer-parallel shortening to fold tightening, using mesostructures: lessons from the Apennines, Pyrenees, and Rocky Mountains, Solid Earth, 12, 2145–2157, https://doi.org/10.5194/se-12-2145-2021, 2021.

Lamarche, J., Lavenu, A. P., Gauthier, B. D., Guglielmi, Y., and Jayet, O.: Relationships between fracture patterns, geodynamics and mechanical stratigraphy in Carbonates (South-East Basin, France), Tectonophysics, 581, 231–245, https://doi.org/10.1016/j.tecto.2012.06.042, 2012.

Lander, R. H. and Laubach, S. E.: Insights into rates of fracture growth and sealing from a model for quartz cementation in fractured sandstones, Geological Society of America Bulletin, 127, 516–538, https://doi.org/10.1130/B31092.1, 2015.

Lavenu, A. P. and Lamarche, J.: What controls diffuse fractures in platform carbonates? Insights from Provence (France) and Apulia (Italy), Journal of Structural Geology, 108, 94–107, https://doi.org/10.1016/j.jsg.2017.05.011, 2018.

Lee, S. H., Lough, M. F., and Jensen, C. L.: Hierarchical modeling of flow in naturally fractured formations with multiple length scales, Water Resources Research, 37, 443–455, https://doi.org/10.1029/2000WR900340, 2001.

Lismonde, B.: Le réseau de la Diau, Karstologia : revue de karstologie et de spéléologie physique, 1, 9–18, https://doi.org/10.3406/karst.1983.2034, 1983.

https://doi.org/10.5194/egusphere-2025-4175
Preprint. Discussion started: 12 September 2025

Looser, N., Madritsch, H., Guillong, M., Laurent, O., Wohlwend, S., and Bernasconi, S. M.: Absolute Age and Temperature Constraints on Deformation Along the Basal Décollement of the Jura Fold-and-Thrust Belt From Carbonate U-Pb Dating and Clumped Isotopes, Tectonics, 40, e2020TC006 439, https://doi.org/10.1029/2020TC006439, 2021.

Lorenz, J. C. and Cooper, S. P.: Atlas of natural and induced fractures in core, John Wiley & Sons, 2017.

Maerten, L., Gillespie, P., and Daniel, J.-M.: Three-Dimensional Geomechanical Modeling for Constraint of Subseismic Fault Simulation, AAPG Bulletin, 90, 1337–1358, https://doi.org/10.1306/03130605148, 2006.

Maerten, L., Maerten, F., Lejri, M., and Gillespie, P.: Geomechanical Paleostress Inversion Using Fracture Data, Journal of Structural Geology, 89, 197–213, https://doi.org/10.1016/j.jsg.2016.06.007, 2016.

Marro, A., Hauvette, L., Borderie, S., and Mosar, J.: Tectonics of the Western Internal Jura Fold-and-Thrust Belt: 2D Kinematic Forward Modelling, Swiss Journal of Geosciences, 116, 10, https://doi.org/10.1186/s00015-023-00435-2, 2023.

Masson, M.: Le karst du Parmelan, Haute-Savoie, relations fracturation-karstification, Karstologia : revue de karstologie et de spéléologie physique, 5, 3–8, https://doi.org/10.3406/karst.1985.2081, 1985.

Mauldon, M., Dunne, W., and Rohrbaugh, M.: Circular Scanlines and Circular Windows: New Tools for Characterizing the Geometry of Fracture Traces, Journal of Structural Geology, 23, 247–258, https://doi.org/10.1016/S0191-8141(00)00094-8, 2001.

Medici, G., Ling, F., and Shang, J.: Review of Discrete Fracture Network Characterization for Geothermal Energy Extraction, Frontiers in Earth Science, 11, 1328 397, https://doi.org/10.3389/feart.2023.1328397, 2023.

Moscariello, A.: Exploring for Geo-Energy Resources in the Geneva Basin (Western Switzerland): Opportunities and Challenges, Swiss Bulletin für angewandte Geologie, 24, 105–124, http://archive-ouverte.unige.ch/unige:131617, 2019.

Moss, S.: Organic Maturation in the French Subalpine Chains: Regional Differences in Burial History and the Size of Tectonic Loads, Journal of the Geological Society, 149, 503–515, https://doi.org/10.1144/gsjgs.149.4.0503, 1992.

Pascal, C.: Paleostress inversion techniques: Methods and applications for tectonics, Elsevier, 2021.

Peacock, D., Sanderson, D., and Rotevatn, A.: Relationships between fractures, Journal of Structural Geology, 106, 41–53, https://doi.org/10.1016/j.jsg.2017.11.010, 2018.

Peacock, D. C., Sanderson, D. J., Bastesen, E., Rotevatn, A., and Storstein, T. H.: Causes of Bias and Uncertainty in Fracture Network Analysis, Norwegian Journal of Geology, https://doi.org/10.17850/njg99-1-06, 2019.

Peacock, D. C. P., Sanderson, D. J., and Leiss, B.: Use of Analogue Exposures of Fractured Rock for Enhanced Geothermal Systems, Geosciences, 12, 318, https://doi.org/10.3390/geosciences12090318, 2022.

Petit, J.-P., Chemenda, A. I., Minisini, D., Richard, P., Bergman, S. C., and Gross, M.: When Do Fractures Initiate during the Geological History of a Sedimentary Basin? Test Case of a Loading-Fracturing Path Methodology, Journal of Structural Geology, 164, 104 683, https://doi.org/10.1016/j.jsg.2022.104683, 2022.

Price, N.: Fault and joint development in brittle and semi-brittle rock. [., Pergamon, Oxford, 1966.

Rusillon, E.: Characterisation and rock typing of deep geothermal reservoirs in the Greater Geneva Basin (Switzerland & France), Ph.D. thesis, Université de Genève, https://doi.org/10.13097/ARCHIVE-OUVERTE/UNIGE:105286, 2017.

Schegg, R. and Leu, W.: Analysis of Erosion Events and Palaeogeothermal Gradients in the North Alpine Foreland Basin of Switzerland, Geological Society, London, Special Publications, 141, 137–155, https://doi.org/10.1144/GSL.SP.1998.141.01.09, 1998.

Simpson, R. W.: Quantifying Anderson's Fault Types, Journal of Geophysical Research: Solid Earth, 102, 17 909–17 919, https://doi.org/10.1029/97JB01274, 1997.

https://doi.org/10.5194/egusphere-2025-4175
Preprint. Discussion started: 12 September 2025

Smeraglia, L., Looser, N., Fabbri, O., Choulet, F., Guillong, M., and Bernasconi, S. M.: U–Pb Dating of Middle Eocene–Pliocene Multiple Tectonic Pulses in the Alpine Foreland, Solid Earth, 12, 2539–2551, https://doi.org/10.5194/se-12-2539-2021, 2021.

Smeraglia, L., Fabbri, O., Choulet, F., Jaggi, M., and Bernasconi, S. M.: The Role of Thrust and Strike-Slip Faults in Controlling Regional-Scale Paleofluid Circulation in Fold-and-Thrust Belts: Insights from the Jura Mountains (Eastern France), Tectonophysics, 829, 229 299, https://doi.org/10.1016/j.tecto.2022.229299, 2022.

Sommaruga, A., Mosar, J., Schori, M., and Gruber, M.: The Role of the Triassic Evaporites Underneath the North Alpine Foreland, in: Permo-Triassic Salt Provinces of Europe, North Africa and the Atlantic Margins, pp. 447–466, Elsevier, ISBN 978-0-12-809417-4, https://doi.org/10.1016/B978-0-12-809417-4.00021-5, 2017.

Strasser, A., Charollais, J., Conrad, M. A., Clavel, B., Pictet, A., and Mastrangelo, B.: The Cretaceous of the Swiss Jura Mountains: An Improved Lithostratigraphic Scheme, Swiss Journal of Geosciences, 109, 201–220, https://doi.org/10.1007/s00015-016-0215-6, 2016.

Torabi, A. and Berg, S. S.: Scaling of fault attributes: A review, Marine and Petroleum Geology, 28, 1444–1460, https://doi.org/10.1016/j.marpetgeo.2011.04.003, 2011.

Tutuarima, F., Cecchetti, E., Abels, H., Bertotti, G., and Bruna, P.: Main controls on natural fracture distribution in the Lower Triassic sandstones of the West Netherlands Basin, in: 84th EAGE Annual Conference & Exhibition, pp. 1–5, European Association of Geoscientists & Engineers, Vienna, Austria,, https://doi.org/10.3997/2214-4609.2023101051, 2023.

Watkins, H., Bond, C. E., Healy, D., and Butler, R. W. H.: Appraisal of Fracture Sampling Methods and a New Workflow to Characterise Heterogeneous Fracture Networks at Outcrop, Journal of Structural Geology, 72, 67–82, https://doi.org/10.1016/j.jsg.2015.02.001, 2015a.

Watkins, H., Butler, R. W., Bond, C. E., and Healy, D.: Influence of structural position on fracture networks in the Torridon Group, Achnashellach fold and thrust belt, NW Scotland, Journal of Structural Geology, 74, 64–80, https://doi.org/10.1016/j.jsg.2015.03.001, 2015b.

Williams, J. H. and Johnson, C. D.: Acoustic and optical borehole-wall imaging for fractured-rock aquifer studies, Journal of Applied Geophysics, 55, 151–159, https://doi.org/10.1016/j.jappgeo.2003.06.009, 2004.

Zang, A., Oye, V., Jousset, P., Deichmann, N., Gritto, R., McGarr, A., Majer, E., and Bruhn, D.: Analysis of induced seismicity in geothermal reservoirs – An overview, Geothermics, 52, 6–21, https://doi.org/10.1016/j.geothermics.2014.06.005, 2014.

Zarian, P. and N. Dymmock, S.: Conceptual Uncertainty in Geological Interpretation of Borehole Image Logs, in: 72nd EAGE Conference and Exhibition incorporating SPE EUROPEC 2010, European Association of Geoscientists & Engineers, Barcelona, Spain,, ISBN 978-90-73781-86-3, https://doi.org/10.3997/2214-4609.201400973, 2010.